Procedure of Data Processing for the Improvement of Failure Time Prediction of a Landslide Based on the Velocity and Acceleration of the Displacement

Imaya Ariyarathna and Katsuo Sasahara

Abstract

Time prediction methods based on monitoring surface displacement (SD) are effective for early warning against shallow landslides. However, failure time prediction by Fukuzono's original inverse-velocity (INV) method is less accurate due to variation in the inverse-velocity $(1/v)$ caused by noise in the measured SD, which amplifies the fluctuation in the resultant $1/v$. Therefore, the present study incorporates pre-analysis to acquire better prediction by reducing the effect of noise on the measured SD. The data extraction (DE) and moving average (MA) methods are used to filter the measured SD for better smoothing of $1/v$. The root mean square error ($RMSE$) and determining factor (f) values are used to select the optimum SD interval (Δx) in the DE method. The $RMSE$ and f values are used to evaluate the reproducibility of the measured data and the scattering in the relationship between velocity and acceleration in an orderly. The data, treated by the DE and MA methods, are utilized to predict the failure time based on the INV method and the relationship between velocity and acceleration on a logarithmic scale (VAA) method. Accordingly, Δx gives the smallest sum of the normalized $RMSE$ and normalized $(1-f)$, which offers a better prediction. When the SD at failure changes, Δx is changed. The best prediction is obtained by DE preprocessing with the VAA method because it minimizes the effect of the individual $1/v$ by reducing the scatter in the relationship between velocity and acceleration. However, the time prediction using data processed by the MA method shows poor prediction due to some scattering of the inverse velocity. In some cases, the prediction by the VAA method using MA data provides better prediction than the results of the INV method.

I. Ariyarathna
Life Environment Science, Ehime University, Matsuyama, Japan

K. Sasahara (✉)
Research and Education Faculty, Kochi University, Kochi, Japan
e-mail: sasahara@kochi-u.ac.jp

1 Introduction

The time prediction of a landslide occurrence is an important task for early warning against landslide disasters, but there is still uncertainty about its precision. However, slope scale prediction is a necessity in the framework of landslide risk reduction. In this regard, prediction based on monitoring displacement data is generally used in practice. Displacement monitoring in indoor model slopes and field experiments using a rainfall simulator have been adopted in recent studies related to shallow landslide failure mechanisms and the forecast time of failure for early warning. For example, Fukuzono (1985) monitored the surface displacement (SD) using extensometers on large-scale indoor model slopes. Furthermore, Moriwaki et al. (2004) conducted the experiments using a full-scale model slope by monitoring the SD with displacement meters. Ochiai et al. (2021) reported the monitoring displacement using extensometers of a field experiment on a natural slope in the city of Futtsu, Chiba Prefecture.

Many researchers have adopted time prediction methods based on monitoring the displacement of slopes (Saito 1965; Fukuzono 1985; Varnes 1982; Voight 1988; Crosta and Agliardi 2003; Rose and Hungr 2007). As mentioned above, the prediction method of the onset of landslide is based on the monitoring of slopes, which is based on the relationship between the time and SD of a slope before the failure occurs, as shown in Fig. 1. Accordingly, the time variation in creep behavior consists of three phases, namely, primary creep, secondary creep and tertiary creep. Among the time prediction methods adopted to date, the method proposed by Fukuzono (1985) has been widely adopted in practice due to its simplicity and convenience of use. He proposed a relationship between the velocity and acceleration of SD

Primary creep
(Decreasing
velocity)

Tertiary creep
(Increasing velocity)

Secondary creep
(Constant velocity)

SD
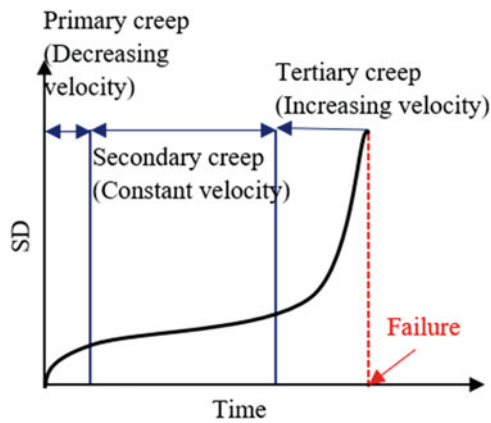
Failure

Time

Fig. 1 Relation between time and SD of the soil before failure under constant stress conditions (Saito 1965)

just before failure (for the tertiary creep stage) in a large-scale model slope under sprinkling water, as shown in Eq. 1.

$$\left(\frac{dv}{dt}\right) = a \cdot v^{\alpha} \qquad (1)$$

where v and t are the velocities of the SD and corresponding times, respectively. In addition, a and α are the experimental constants that result from the intercept on the vertical axis and gradient of the relationship line, respectively, when the velocity and acceleration of the SD data are plotted over time (Fig. 2).

Based on the above relationship, he introduced a prediction method called inverse-velocity method (INV), which

1E+03

Acceleration (cm/h/h)

1E+02

1E+01

α

1E+00

1E-02 1E+01 1E+02 1E+03
Velocity (cm/h)

1E-01

1E-02

a
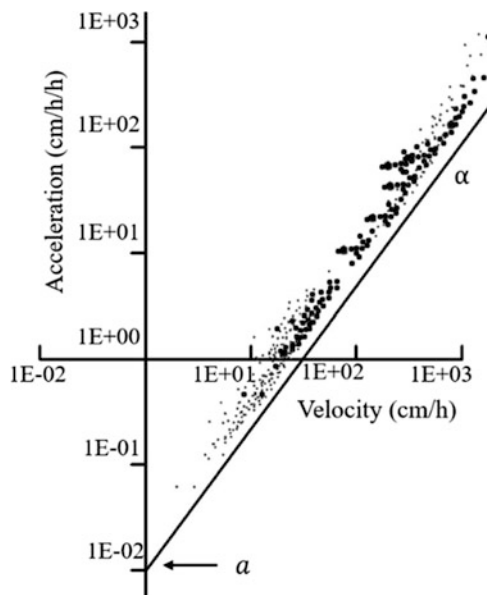
Fig. 2 Relationship between the velocity and acceleration of the SD (Fukuzono 1985)

was created by integrating the relationship between the velocity and acceleration of SD by time just prior to failure (Eq. 2).

$$\frac{1}{v} = \{a(\alpha-1)\}^{\frac{1}{\alpha-1}}(t_r - t)^{\frac{1}{\alpha-1}} \qquad (2)$$

where t_r is the predicted failure time. Fukuzono (1985) noted that the inverse velocity reached zero just before failure. Therefore, the failure time of a slope by the INV method could be determined by extrapolating the resultant curves to cross the time axis.

The past literature reveals that many researchers have adopted the INV method to forecast the failure time of landslides and that some of them achieved precise prediction, while some of them did not succeed completely. For example, Carla et al. (2019) predicted the failure time of a natural rockfall by the GBInSAR method using the INV method, and they conveyed that the INV method gives precise results. Mazzanti et al. (2015) highlighted that an improved version of the INV method called ADF (average data Fukuzono) is necessary to achieve the best results. ADF incorporates the moving average of the displacement data over time and effectively minimizes the prediction error due to scattering of inverse-velocity values. Furthermore, Zhou et al. (2020) emphasized that the time prediction effectiveness using INV is limited for actual landslides and that accuracy can be improved by introducing controllable variables. He proposed the modified INV method, which improves the accuracy of the predicted failure time by avoiding earlier prediction than actual failure time. That report noted that the forecasting effectiveness of the INV methods directly depends on the quality of the measured displacement data. Accordingly, the time prediction by Fukuzono's original INV may succeed in some cases but not in others because the results are widely affected by the quality of the measured data, as the displacement noise amplifies the resultant velocity. If the error in displacement data is not so considerable, the velocity variation, which is calculated using the same displacement data, becomes higher. This results in causes several peak values with up and down variations in velocities over time before failure. Hence, the present study focuses on improving the failure prediction by minimizing the influences of the inverse velocity fluctuation by introducing the preprocessing of displacement data before the prediction.

2 Methodology

2.1 Methods for Raw Data Preprocessing

Data preprocessing is introduced to obtain a better prediction, which reduces the sudden fluctuation of $1/v$ values by decreasing the effect of noise on the measured SD. Two

approaches called the data extraction method (DE) and moving average method (MA) are utilized in the present study.

2.1.1 Data Extraction Method (DE)

The DE method is carried out to determine the optimal displacement interval (Δx) for extracting the data to predict the failure time, which minimizes the scattering of $1/v$ values by avoiding the noise of the measured SD. The root mean square error (*RMSE*) and determining factor (f) values are used as supportive parameters to evaluate the reproducibility of the measured data and scattering in the relationship between velocity and acceleration in order to select Δx for the DE method. The *RMSE* values are calculated by Eq. 3.

$$RMSE = \sqrt{\frac{1}{N}\sum_{i=1}^{N}(F_1 - A_1)^2} \qquad (3)$$

where N is the total number of the data, F_i is the measured SD at time t_i, A_i is the extracted SD at time t_i, and $(F_i - A_i)$ indicates an error between the measured and extracted SD. Suppose there are no data at the time t_i for the extracted data. In that case, data corresponding to t_i are projected by considering the proportional distribution of the extracted data before and after time t_i, as shown in Fig. 3. Generally, when the data extracting SD interval (ΔSD) is increased, the reproducibility of the measured data is decreased, and the calculated *RMSE* values become larger.

The f values measure how well the regression line fits with the velocity and acceleration data on a logarithmic scale (Fig. 2). The linear regression line was obtained using Microsoft Excel for the relationship between velocity and acceleration on a logarithmic scale utilized to get the f values. It expresses how much percentage of the total variation in acceleration (vertical axis) is described by the velocity variation (horizontal axis) in the relationship between velocity and acceleration on a logarithmic scale which is always between 0.0 to 1.0. A value of 1.0 indicates
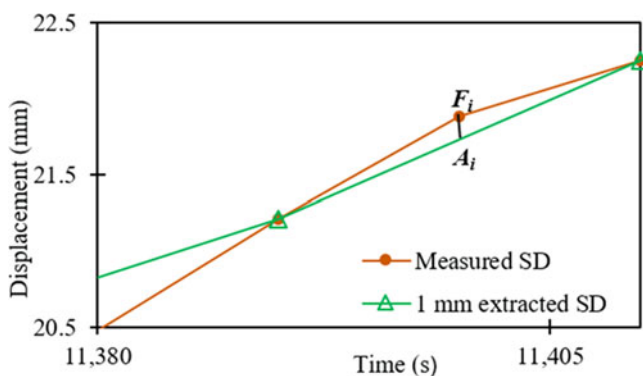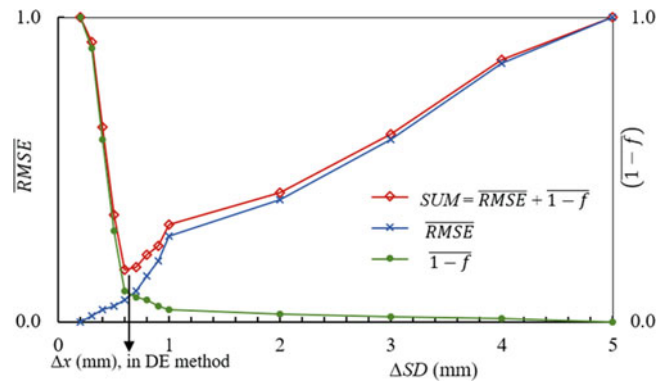

Fig. 4 $\overline{RMSE}$ and $(\overline{1-f})$ value variation with different data extracting SD interval (ΔSD)

a higher relationship strength. It means the lowest value of $(1\text{-}f)$ gives the lowest scattering. However, calculated *RMSE* and $(1\text{-}f)$ are not in the same range, which causes the weight ratio between *RMSE* and $(1\text{-}f)$, is changed depending on the ΔSD. So, in the case of *RMSE*, though the minimum value is zero, the maximum value is changed by more than 1.0. In that case, the maximum and minimum value difference is equal to the one and calculate all values within the range of 0.0 to 1.0 as normalized *RMSE* ($\overline{RMSE}$). So, both values are normalized into the same range, 0.0 to 1.0, assigning the weight ratio 1:1 between *RMSE* and $(1\text{-}f)$, as shown in Fig. 4. The ΔSD increases, the discrepancy between measured and extracted.
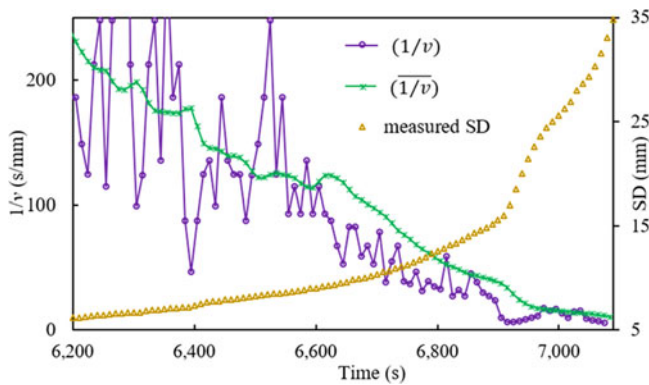
data increases, and scattering in the relationship between the velocity and acceleration decreases. Considering the optimum displacement interval (Δx), it gives at the lowest summation of ($\overline{RMSE}$) and normalized $(1\text{-}f)$, $(\overline{1-f})$.

2.1.2 Moving Average (MA) Method

The moving average inverse velocity ($\overline{1/v}$) values (calculated by considering consecutive $1/v$ values) are used to smooth the time variation of $1/v$ in the MA method. In this regard, we calculate ($\overline{1/v}$) by considering different consecutive values and select the best consecutive value, which gives the best smoothing time variation of $1/v$. The ($\overline{1/v}$) at time step, l, is calculated using Eq. 4.

$$\left(\overline{1/v}\right)_l = \frac{(1/v)_l + (1/v)_{l-1} + \ldots (1/v)_{l-(n-1)}}{n} \qquad (4)$$

where n is the number of time steps, l is the present time step, and $1/v$ is the inverse velocity value at the corresponding time step. As an example, when calculating the ($\overline{1/v}$) by considering two ($n = 2$) $1/v$ values, ($\overline{1/v}$) is defined as the summation of the $1/v$ values at present and previous time steps divided by two. As shown in Fig. 5, if the disturbance of SD is not significant, the $1/v$ variation calculated using the same SD

Fig. 3 The comparison of the time variation of displacement for the measured SD and SD extracted in 1 mm intervals

Fig. 5 Time variation of the inverse velocity derived from both the measured $1/v$ and smoothed inverse velocity $(\overline{1/v})$ and the SD

becomes higher. However, the individual fluctuation is lower when considering $(\overline{1/v})$, which gives a smoother curve.

2.2 Prediction of the Failure Time

2.2.1 Calculation of Velocity and Acceleration Values

The calculation of the velocity and acceleration from the measured SD and time data is explained below. First, the velocity is defined as the SD difference between the previous and present time steps divided by the corresponding time step difference. Second, the acceleration is defined as the velocity difference between the previous and present time steps divided by the corresponding time step difference.

2.2.2 Failure Prediction from Fukuzono's Original Inverse-Velocity (INV) Method

The INV method is based on the relationship between $1/v$ and time, which reaches zero just before failure. Therefore, the failure time prediction can be predicted by extrapolating resultant curves to cross the time axis, which is given by the time differentiation $1/v$ in Eq. 2 and some arrangement to produce the ratio of $1/v$ to the increment of the inverse velocity, as shown in Eq. 5.

$$\left(\frac{1}{v}\right) \Big/ \left(\frac{d(1/v)}{dt}\right) = -(\alpha - 1)(t_r - t) \quad (5)$$

The failure time can be calculated using the ratio of the $1/v$ to its increment ratio at two different times, as shown in Eq. 6, which is the process of the INV method initially proposed by Fukuzono (1985).

$$t_r = \frac{t_2(1/v)_1/(d(1/v)/dt)_1 - t_1(1/v)_2/(d(1/v)/dt)_2}{(1/v)_1/(d(1/v)/dt)_1 - (1/v)_2/(d(1/v)/dt)_2} \quad (6)$$

2.2.3 Failure Prediction from the Relationship Between Velocity and Acceleration (VAA) Method

The failure time prediction by the VAA method can be derived from the rearrangement of Eq. 2 to Eq. 7.

$$t_r = t + \frac{1}{a(\alpha - 1)} \left(\frac{1}{v}\right)^{\alpha - 1} \quad (7)$$

The failure time can be derived by substituting the present time (t) and corresponding inverse-velocity values $(1/v)$ with a and α values into Eq. 7. The a and α values are derived from the relationship between velocity and acceleration on a logarithmic scale from linear regression analysis as shown in Fig. 2.

2.3 Landslide Field Experiment on a Natural Slope in Futtsu, Chiba Prefecture

2.3.1 Experimental Setups

A landslide field experiment on a natural slope in Futtsu, Chiba Prefecture, was conducted on 12 December 2018 using a rainfall simulator as requested by NHK, Nippon Hoso Kyokai (Japan Broadcast Corporation). The experimental site was sparsely forested with hardwoods with a slope of approximately 40 degrees. The ground surface was a smooth slope surface covered with Simon bamboo and ivy, and part of the lower edge of the slope had previously been quarried for sand. The behavior of the slope was monitored and filmed with multiple cameras during the main experiment.

The grain size distribution of the surface soil layer is shown in Fig. 6. Accordingly, the majority of the soil consists of sand particles (75%), and the rest are silts particles (23%) and clay particles (2%). The mean diameter of the soil particles is 0.1509 mm. The physical properties of the soil are shown in Table 1. Accordingly, soil particle density is 2.574 g/cm^3, and the minimum and maximum density of the soil is between 1.082 to 1.361 g/cm^3. The thickness of the surface soil layer was approximately 1 m based on the results of a portable penetration test (Japanese Geotechnical Society, 2017) using a number of blows (10 cm penetration) with a 5 kg weight dropped from a height of 50 cm. During the experiment, artificial rainfall was supplied to an area 10 m long and 10 m wide. The pre-experiment with a precipitation intensity of 140 mm/h was conducted for around 1 h on 11 December 2018 to fine-tune the distribution of the
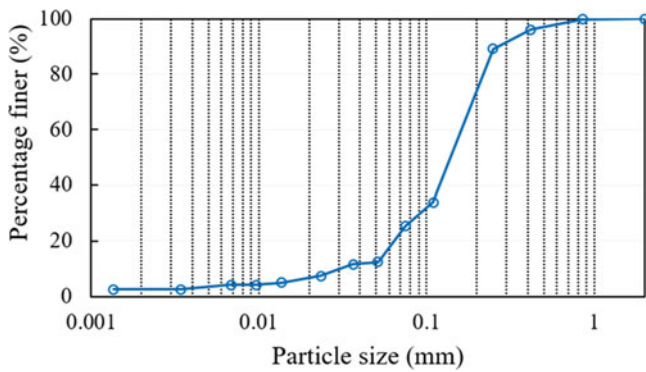
Fig. 6 Grain size distribution of the surface soil at the experimental site

precipitation. A total of six extensometers at three locations along two survey lines were installed (Fig. 7a). Extensometers 1, 2, and 3 were placed on line 1 (Fig. 7b), and the others were placed on line 2. A detailed explanation of the experiment can be found in Ochiai et al. (2021).

2.4 In-door Small-scale Model Slope Experiment

2.4.1 Experimental Setups

The data obtained from the in-door small-scale model slope at Kochi University was utilized in this study. Figure 8a, b show the lateral view and longitudinal section of the small-scale model slope and monitoring device arrangement, respectively, at Kochi University. The model was 110 cm and 55 cm long, respectively, in slope and horizontal sections with a width of 60 cm and depth of 12 cm. The model slope's base plate consisted of steel blades with a height of 1 cm and length equal to the width of the base plate by every 20 cm from 10 cm to 90 cm from the upper boundary in the slope section and from 7.5 cm to 47 cm from the end of the lower boundary in the horizontal section of the model slope and coarse sand to prevent sliding between the soil and the base plate. The model slope's dry unit weight, and upper slope inclination were 1.32 g/cm^3, and 40 degrees, respectively. The experiment was carried out under sprinkling water with constant discharge from the rainfall simulator, and its intensity was expressed in mm/h. Accordingly, 108 mm/h rainfall

intensity was used for the experiment. Well-graded sand with fine (The Japanese Geotechnical Society, 2015) with a grain size distribution shown in Fig. 9 was used to prepare the model slope and other physical properties are shown in Table 2.

The SD was measured using three displacement gauges fixed at the lateral boundary of the flume from the distance of 25 cm, 55 cm, and 80 cm away from the upper boundary of the flume. The SD data and their corresponding time at the 55 cm (middle) displacement gauge were utilized for the analysis. The displacement gauge's capacity and resolution are 100 mm and 0.2 mm, respectively and data were logged every 10 s by a data logger. The displacement gauges are the SDP-100CT, strain-generating cantilever type displacement transducer from the Tokyo Sokki Kenkyujo Company, and measure the tension displacement using a hook bolt.

3 Results

This section presents only the results corresponding to extensometer No. 5 (orange colour in Fig. 10) in the natural slope experiment, Futtsu, and the displacement gauge, installed at 55 cm from the upper boundary of the model slope in the small-scale model slope experiment.

3.1 Experimental Results

A landslide occurred at field experiment on a natural slope in Futtsu, after 4 h and 25 min of rainfall with an intensity of 140–300 mm/h, and the depth of the landslide was approximately 1 m, according to Ochiai et al. (2021). Furthermore, Fig. 7b shows the cross-section before (black colour line) and after (pink colour line) failure and reveals that the failure was a sliding-type landslide.

Although six extensometers were installed on the experimental slope, only Nos. 1 and 5 were within the landslide mass, and the others were out of the landslide area. Therefore, the SD measured at their corresponding times by extensometers Nos. 1 and 5 was used for the present study. Extensometers No. 1 (blue colour) and No. 5 (orange colour) show the movement along the surface approximately 275 mm

Table 1 Physical properties of the natural slope in Futtsu experiment

Soil particle density (g/cm^3)	2.574
Minimum density (g/cm^3)	1.082
Maximum density (g/cm^3)	1.361
Minimum void ratio of the soil, e_{min}	0.891
Maximum void ratio of the soil, e_{max}	1.379
Coefficient of uniformity	2.3

Fig. 7 (**a**) Front view of the natural slope in Futtsu and arrangement of displacement gauges, and (**b**) longitudinal section along line 1 at experimental slope at Futtsu (with the locations of displacement gauges Nos. 1, 2, and 3)
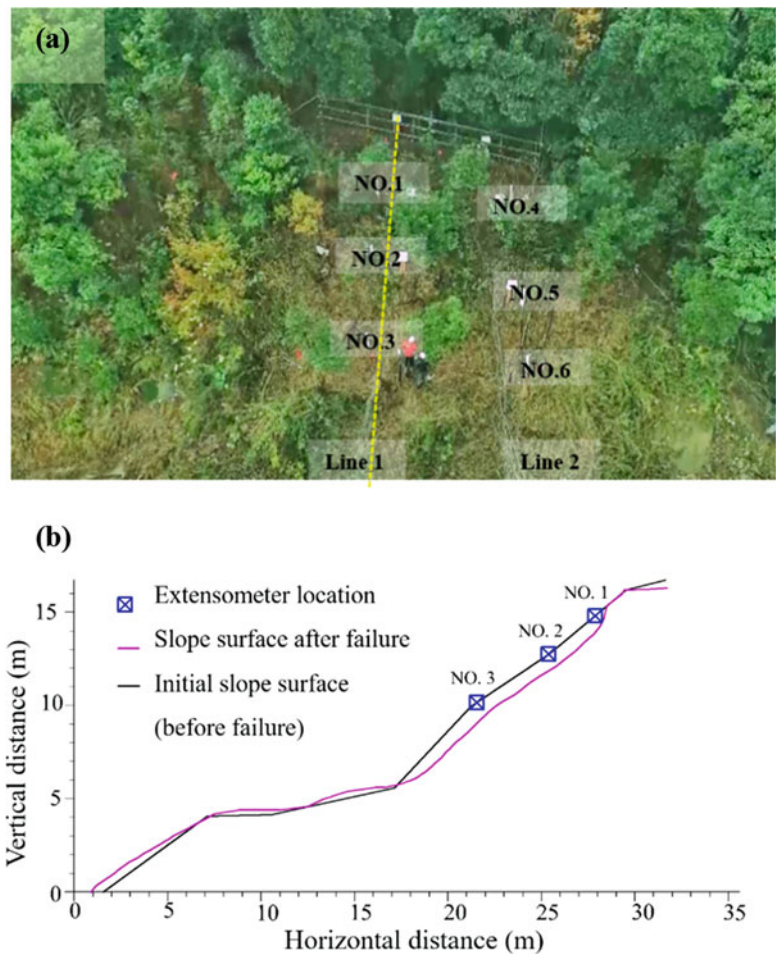
to 204 mm just before the failure (Fig. 10). Figure 11 shows the slope geometry after the failure. The landslide initiation boundary is demarcated using yellow colour dotted line and red color arrows showing the debris moving direction. A closer view of the landslide crest area shows in the upper left corner of Fig. 11. Ochiai et al. (2021) mentioned that the groundwater levels on the upper slope increased again along with the accelerated movements in the middle slope, which led to the landslide initiation. The failure was initiated after the 7,090 s in the in-door small-scale model slope experiment and it was a sliding type failure.

3.2 Data Preprocessing

3.2.1 Data Extraction Method (DE)

Figure 12a, b show $\overline{RMSE}$ and $(\overline{1-f})$ values variation with the different SD intervals (ΔSD) in the DE method for orderly natural slope experiment, Futtsu, and small-scale model slope. In the natural slope experiment and small-scale model slope, recorded SD and time at failure were 204.4 mm and 34.79 mm, and 22,680 s and 7090 s, respectively. According to the results of the DE method, 3.0 mm

and 1.0 mm SD intervals are the optimum displacement interval (Δx) for data extraction corresponding to the natural slope experiment and small-scale model slope orderly to failure time prediction. The analysis is carried out by selecting a SD interval from 0.1 mm to 1.0 mm by a 0.1 mm difference and then a 1.0 mm interval difference until 10.0 mm for the natural slope experiment and a SD interval from 0.2 mm to 1.0 mm by a 0.1 mm difference and then a 1.0 mm interval difference until 5.0 mm for small-scale model slope. Because the accuracy of the displacement gauge used for the in-door small-scale model slope experiment is 0.2 mm, 0.2 mm is used for the minimum ΔSD value in the DE process.

Figure 12a shows that $\overline{RMSE}$ values gradually increase when the ΔSD is increased except at the 0.1 mm interval and 3.0 mm interval. The calculated $\overline{RMSE}$ at the 3.0 mm interval is a similar value, 0.30, with the 2.0 mm interval. The parameter $(\overline{1-f})$ gradually decreases as the ΔSD increases, but a small increase of less than 0.03 can be observed until 0.8 mm from 0.5 mm. Subsequently, the $(\overline{1-f})$ values suddenly drop until reaching 2.0 mm and then decrease smoothly. However, the sum of $\overline{RMSE}$ and $(\overline{1-f})$ shows the lowest value at
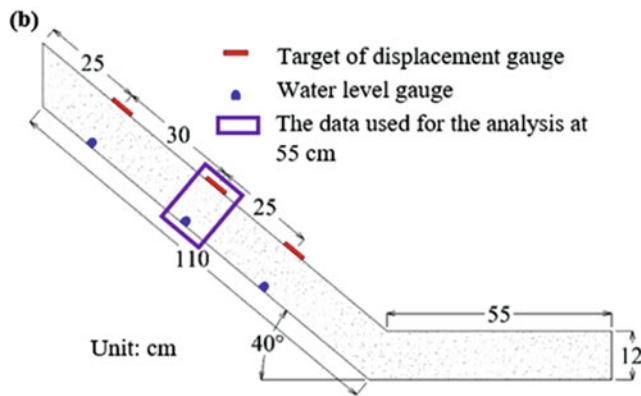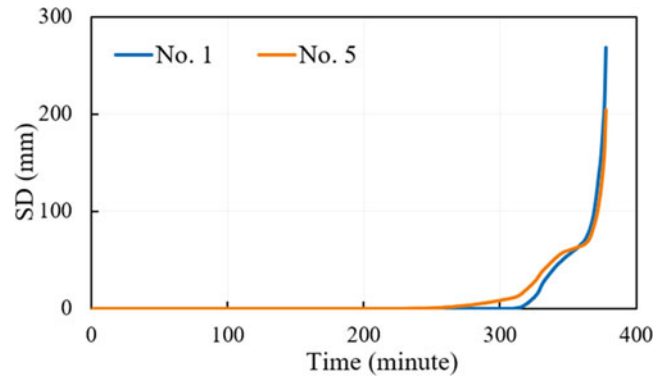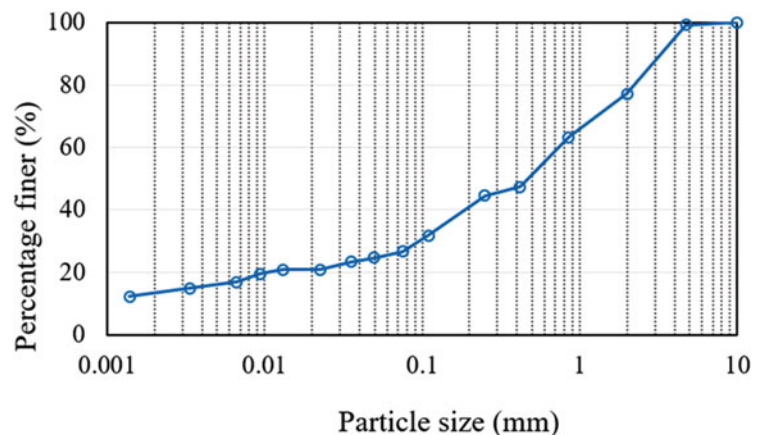
Fig. 8 (**a**) Lateral view of the model slope, (**b**) longitudinal section of the model slope and arrangement of measurement devices at Kochi University

Fig. 10 The time variation of the surface displacement (SD), measured by extensometer Nos. 1 and 5

values suddenly drop from 0.3 mm to 1.0 mm, while showing peak values at 0.6 mm and 0.8 mm. After the 1.0 mm, ΔSD, $\overline{(1-f)}$ values show some fluctuation within the range of 0.0 to 0.19. However, the sum of $\overline{RMSE}$ and $\overline{(1-f)}$ values show the lowest value at 1 mm as 0.16. The 0.9 mm interval also shows a closer value, 0.17 to 1.0 mm, as the sum of $\overline{RMSE}$ and $\overline{(1-f)}$.

3.2.2 Moving Average (MA) Method

Figure 13a, b show the time variation of $1/v$ and $\overline{(1/v)}$, which is calculated by considering the different number of consecutives $1/v$ to select the best smooth time variation of $\overline{(1/v)}$ in the MA method for orderly natural slope experiment, Futtsu and in-door small-scale model slope. Accordingly, moving average velocities are calculated using 2, 5, 10, and 20 consecutives (2MA, 5MA, 10MA, and 20MA). The results reveal that when the considered number of consecutive increases, the smoothness of the resultant time variation $\overline{(1/v)}$ curves is improved, especially just before the failure. Accordingly, the results obtained from the natural slope experiment (Fig. 13a) highlighted that the significant increase of $1/v$ from 19,880 s to 20,990 s and fluctuation until

3.0 mm as 0.37. The 2.0 mm interval also shows a closer value, 0.38 to 3.0 mm, as the sum of $\overline{RMSE}$ and $\overline{(1-f)}$.

Figure 12b shows that $\overline{RMSE}$ and $\overline{(1-f)}$ values increase and decrease in an orderly with increasing the ΔSD, but not gradually, and shows some up and down values. The $\overline{RMSE}$ values increase gradually, with a decreasing value at 0.7 mm and approximately similar at the nearest ΔSD, 0.5 mm and 0.9 mm, with 0.6 mm and 1.0 mm, respectively. $\overline{(1-f)}$

Fig. 9 Grain size distribution of the model slope's soil

21,540 s, instead of decreasing causes, making a peak in the time variation $(\overline{1/v})$ curve.

3.3 Prediction of Failure Time

In the present study, the time remaining to failure $(t_r\text{-}t)$ approaching zero just before failure is considered an indicator for failure prediction. Though the time variation of the predicted failure time (t_r) can be used as an indicator, experimental results reveal that it increases and approaches actual failure time with time instead of the constant time variation of predicted failure time. In that scenario, the time just before the failure cannot be easily identified using the time variation of predicted failure time. In contrast, the time variation $(t_r\text{-}t)$ leads to a more precise prediction.

3.3.1 Prediction Results by the INV Method

Figure 14a, b show the failure time prediction by the INV method using the data processed by the DE method for the natural slope experiment, Futtsu and small-scale model slope experiments in an orderly. Figure 14a contains the time variation of $(t_r\text{-}t)$ by the INV method using the DE processed data by only the data extracting SD intervals (ΔSD), 0.1 mm,

0.6 mm, 3 mm, and 10 mm for the natural slope experiment. It shows that the predicted $(t_r\text{-}t)$ by the INV method using DE data for the natural slope experiment tends to lie along the time axis with some up and down fluctuation in the 0.1 mm extracted data. However, upon comparing the results of higher ΔSD, the prediction shows the values away from the time axis, suggesting that when the ΔSD is higher, the method gives a later prediction. However, the prediction using the INV method and DE data for the natural slope experiment shows negative values throughout the prediction in all ΔSD, which means that the prediction results indicate that slope failure has already occurred during the experiment. Figure 14b presents the time variation of $(t_r\text{-}t)$ by the INV method using the DE processed data by only ΔSD, 0.2 mm, 0.6 mm, 1 mm, and 5 mm for the small-scale model slope experiment. The predicted $(t_r\text{-}t)$ using ΔSD, 0.2 mm, 0.6 mm, and 1 mm shows similar behaviors as the natural slope experiment results. But the predicted $(t_r\text{-}t)$ with the 5 mm interval extraction data shows a gradually decreasing trend with time. It used only the five SD values to predict the failure time from 6000 s to collapse, and among them, two values were negative $(t_r\text{-}t)$ just before the failure (around 6925 s and 6978 s).

Table 2 Physical properties of the model slope

Soil particle density (g/cm^3)	2.651
Maximum density (g/cm^3)	1.733
Minimum density (g/cm^3)	1.344
Minimum void ratio of the soil, e_{min}	0.420
Maximum void ratio of the soil, e_{max}	0.833
Coefficient of uniformity	12.98
Water content of the model slope, w (%)	3.64

Fig. 12 $\overline{RMSE}$ and $(\overline{1-f})$ values variation with the different data extracting SD interval (ΔSD) in the DE method for (**a**) natural slope experiment, Futtsu, and (**b**) in-door small-scale model slope experiment
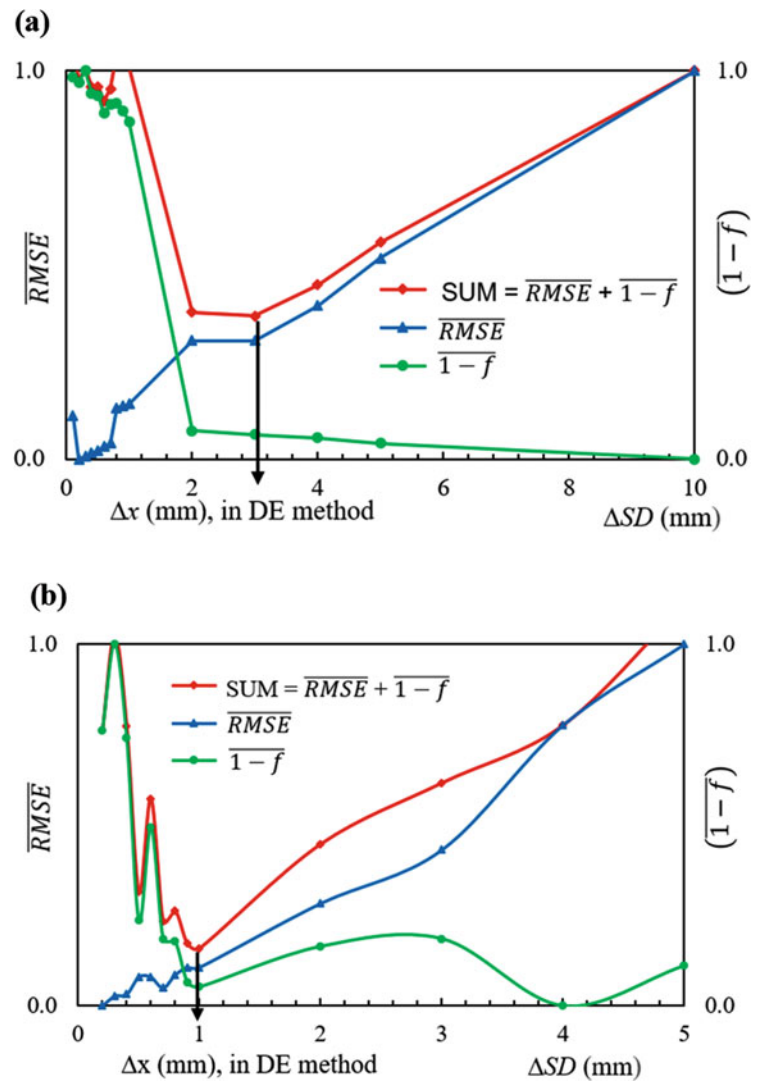

Figure 15a, b show the failure time prediction by the INV method using the data processed by the MA method for the natural slope experiment, Futtsu, and small-scale model slope experiments in an orderly. The predictions were carried out using the MA method by calculating the moving average velocities $(\overline{1/v})$ using 2, 5, 10, and 20 consecutives, respectively, 2MA, 5MA, 10MA, and 20 MA. In this regard, the variation of $(t_r\text{-}t)$ with time is the same pattern in both experiments. The results obtained from the INV method prediction, using MA data, are more scattered than those obtained from the DE data. However, the results from MA data by the INV method prediction show negative values throughout the prediction by the $(\overline{1/v})$ using the different number of consecutives. Therefore, the prediction by the INV method, with both DE and MA data, shows less precision because the results still show scattering and negative values just before failure.

3.3.2 Prediction Results by the VAA Method

Figure 16 shows the time variation of $(t_r\text{-}t)$ by the VAA method from the data processed by the DE method. In order, Fig. 16a, b refer to the time variation of $(t_r\text{-}t)$ for the natural slope experiment, Futtsu, and small-scale model slope experiment just before the failure. The results of the natural slope experiment revealed that the predicted $(t_r\text{-}t)$ is generally decreasing and closer to zero just before failure by the data extracted SD interval (ΔSD) of 0.1 mm, 0.6 mm, 3 mm, and 10 mm (Fig. 16a). The prediction using ΔSD, 0.1 mm, and 0.6 mm show some scattering compared with the results obtained from 3 mm and 10 mm. The fluctuation of time remaining to failure $(t_r\text{-}t)$ from the ΔSD using 3 mm and 10 mm intervals is minimal compared with the other predictions. When comparing the results from 3 mm and 10 mm intervals, the 3 mm interval gives a better linear decreasing trend than the 10 mm interval. Therefore 3 mm

Fig. 13 Time variation of $1/v$ and $(\overline{1/v})$, for, (**a**) natural slope experiment, Futtsu, and (**b**) in-door small-scale model slope experiment (different number of consecutive velocity values, used for calculating $(\overline{1/v})$, considering 2, 5, 10 and 20 adjacent values are referred in orderly 2MA, 5MA, 10MA, and 20MA in the MA method)
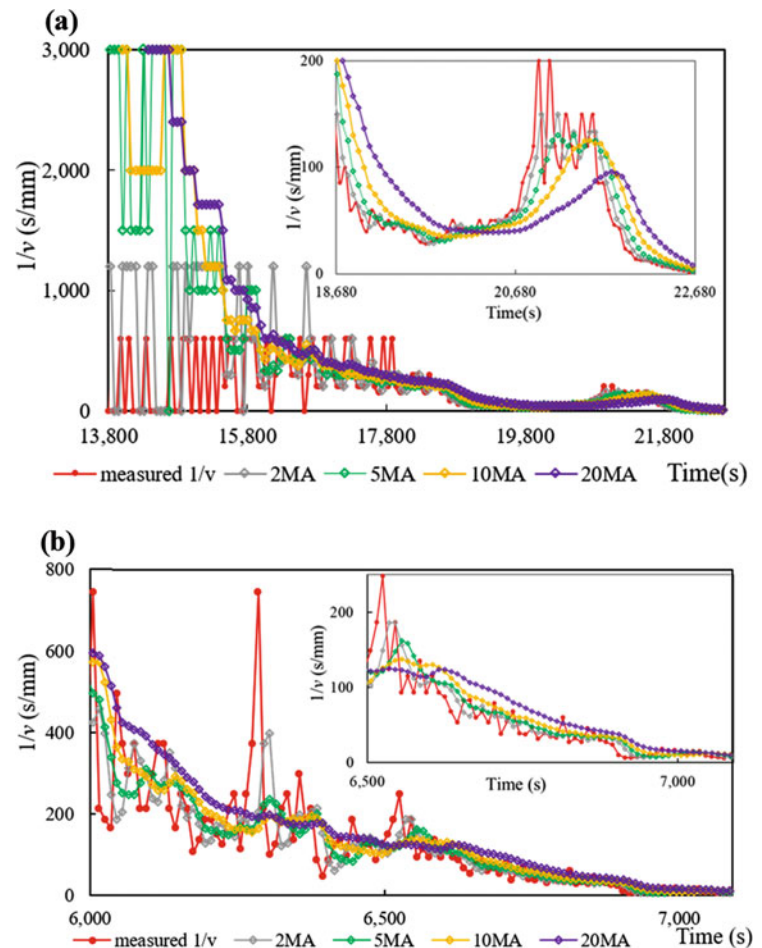

is the optimum displacement interval *(Δx)* for DE corresponding to the natural slope experiment, as it offers the best results for failure prediction by the VAA method. Figure 16b shows the time variation of *(t_r-t)* predicted using *ΔSD,* 0.2 mm, 0.6 mm, 1 mm, and 5 mm, just before the failure. The prediction using 0.2 mm shows some negative predictions, which means that the slope has already collapsed during the experiment monitoring. The *ΔSD*, 0.6 mm, and 5 mm predictions show relatively higher scattering than the 1 mm. The prediction results by 1 mm show the general trend of decreasing with time and getting closer to zero. Therefore 1 mm is *Δx* for DE, corresponding to the small-scale model slope experiment, as it offers the best failure prediction by the VAA method.

Figure 17a, b show the time variation of *(t_r-t)* by the VAA method for the data processed by the MA method in an orderly natural slope experiment, Futtsu, and small-scale model slope experiment, just before the failure. Figure 17a highlights that the VAA method's prediction using the 2MA and 10MA processed data gives the general trend of decreasing *(t_r-t)* while 5MA and 20MA give the predicted *(t_r-t)* with negative values and along the time axis, respectively.

However, the results obtained from the 5MA and 20MA show poor prediction. The predicted *(t_r-t)* obtained from the small-scale model slope experiment (Fig. 17b) highlighted that the VAA method's prediction using the MA method's processed data gives negative predictions, even just before the failure, regardless of the number *(n)* used for calculating the moving average. The time variation of *(t_r-t)* by 5MA processed data shows a general decreasing trend just before the failure.

The VAA method's prediction using the MA shows decreasing trends in the latter time before the failure compared with the results of the VAA method using DE data. On the other hand, the results obtained from the VAA method using the MA show a higher scatter just before the failure, while the VAA method using DE gives relatively less scatter. Furthermore, the prediction given by the VAA method using MA data has uncertainty and depends on the conditions, which could not be ensured in every case. In the natural slope experiment, Futtsu revealed that the time variation of *(t_r-t)* decreases only by 2MA and 10MA processed data, and the small-scale model slope experiment shows a decreasing trend of *(t_r-t)* with time by only 20MA processed data. For

Fig. 14 Time variation of the time remaining to failure (t_r-t) by the INV method using the data processed by DE method for, (**a**) natural slope experiment, Futtsu, and (**b**) in-door small-scale model slope experiment (0.1 mm_DE, 0.2 mm_DE, 0.6 mm_DE, 1 mm_DE, 3 mm_DE, 5 mm_DE, and 10 mm_DE represent the results from the DE by SD intervals of 0.1 mm, 0.2 mm, 0.6 mm, 1 mm, 3 mm, 5 mm, and 10 mm)
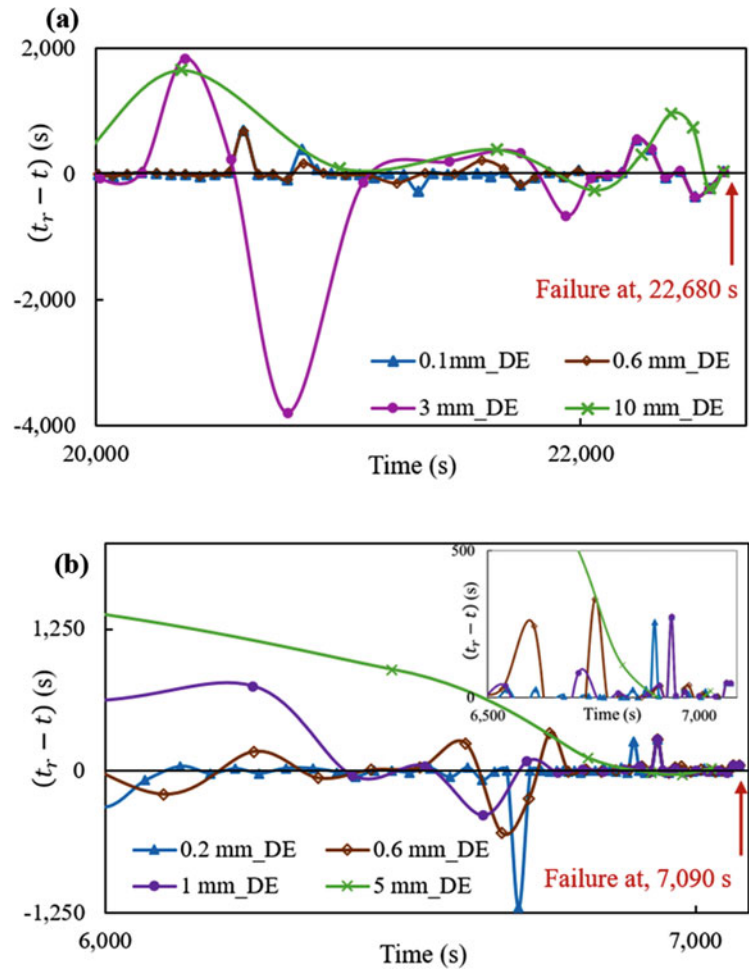
example, if the prediction by the VAA method using 2MA and 10MA gives a decreasing trend, then 5MA gives a poor prediction. Based on the present analysis, the prediction given by the VAA method using 10MA gives a linearly decreasing trend compared to 2MA with the above-explained complications. Therefore, the best prediction is obtained from the VAA method using data processed by the DE method.

The failure time prediction made using the VAA method gives better results than the INV method because it utilizes the linear regression analysis in the relationship between velocity and acceleration and causes less influence from the individual variation of the inverse velocity values. But still, some scattering remained, resulting from the noise of the measured SD. Therefore, the data preprocessing method was introduced to acquire better prediction by reducing the effect of noise on the measured SD. The prediction using DE processed data gives better results than MA processed data. So, time prediction based on the VAA method with DE preprocessing data can be used to monitor the real-time data with better precision than others. The prediction results, the VAA method with DE processed data by comparing with other methods, leads to reduce the fluctuation of predicted

failure time and minimizes the disturbance to decreasing trend. It does not mean all fluctuations can be avoided, but it reduces and improves more than other methods. For example, the prediction by the VAA method using 3 mm extracted data for natural slope experiment, Futtsu, decreasing trend shows two gradients (Fig. 16a pink colour) during its general decreasing trend of predicted time remain to failure (t_r-t) with time. But results are more precise than the others.

4 Conclusions

The present study predicted the failure time using two methods with different preprocessing data methods to evaluate the effectiveness of the preprocessing data methodologies to improve the failure prediction using field experiment data on a natural slope in Futtsu, Chiba Prefecture. During the study, the following conclusions could be drawn.

1. The failure prediction by the VAA method using DE preprocessing gives the best prediction because it minimizes the individual velocity variation. In the process

Fig. 15 Time variation of the time remaining to failure (t_r-t) by the INV method using the data processed by MA method, for, (**a**) natural slope experiment, Futtsu, and (**b**) in-door small-scale model slope experiment
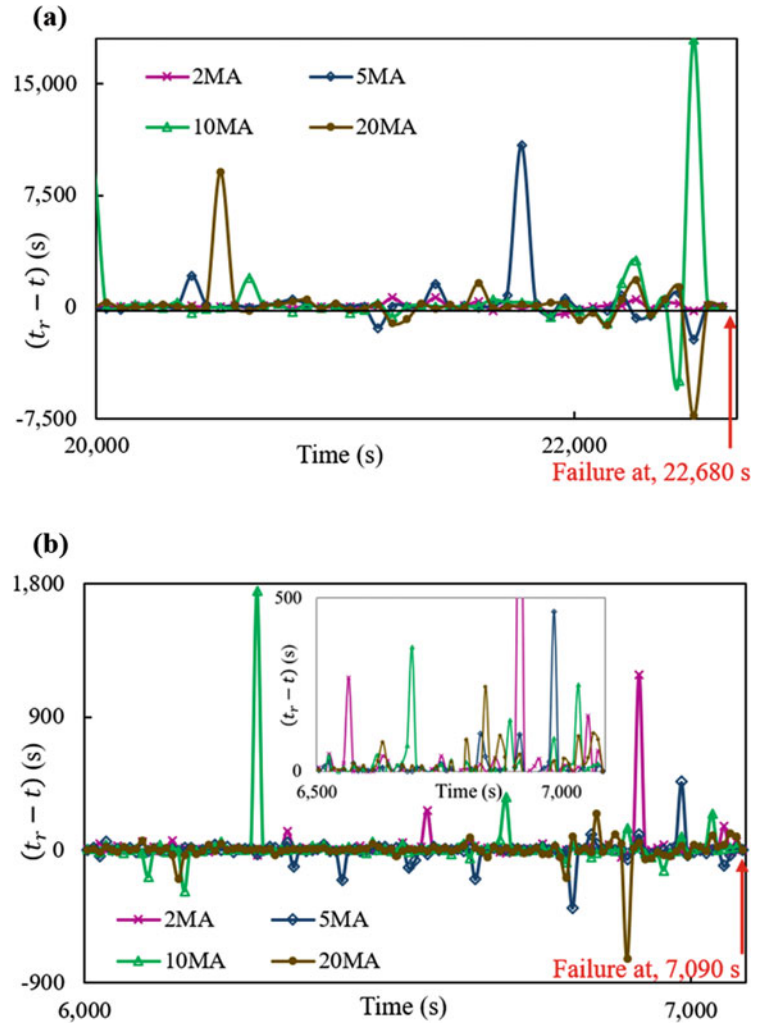

of DE, not only reproducibility but also equal priority is given to reducing the scatter in the relationship between velocity and acceleration.

2. The optimal displacement interval (Δx) by the DE method corresponds to the smallest sum of $\overline{RMSE}$ and $(\overline{1-f})$, which gives the best prediction using the data extracted by the VAA method. The Δx changes depending on the distance moved by the landslide. Therefore, more studies on a different scale of landslides are needed to obtain the relationship between Δx and the moved displacement.

3. Best smoothing of the time variation of the inverse velocity curve is obtained from the moving average inverse velocities calculated by a larger number of consecutive inverse velocities than a small number of consecutive inverse velocities. However, the time prediction using data processed by the MA method shows poor prediction due to some scattering of the inverse velocity.

Fig. 16 Time variation of the time remaining to failure (t_r-t) by the VAA method using the data processed by the DE method for (**a**) natural slope experiment, Futtsu, and (**b**) in-door small-scale model slope experiment
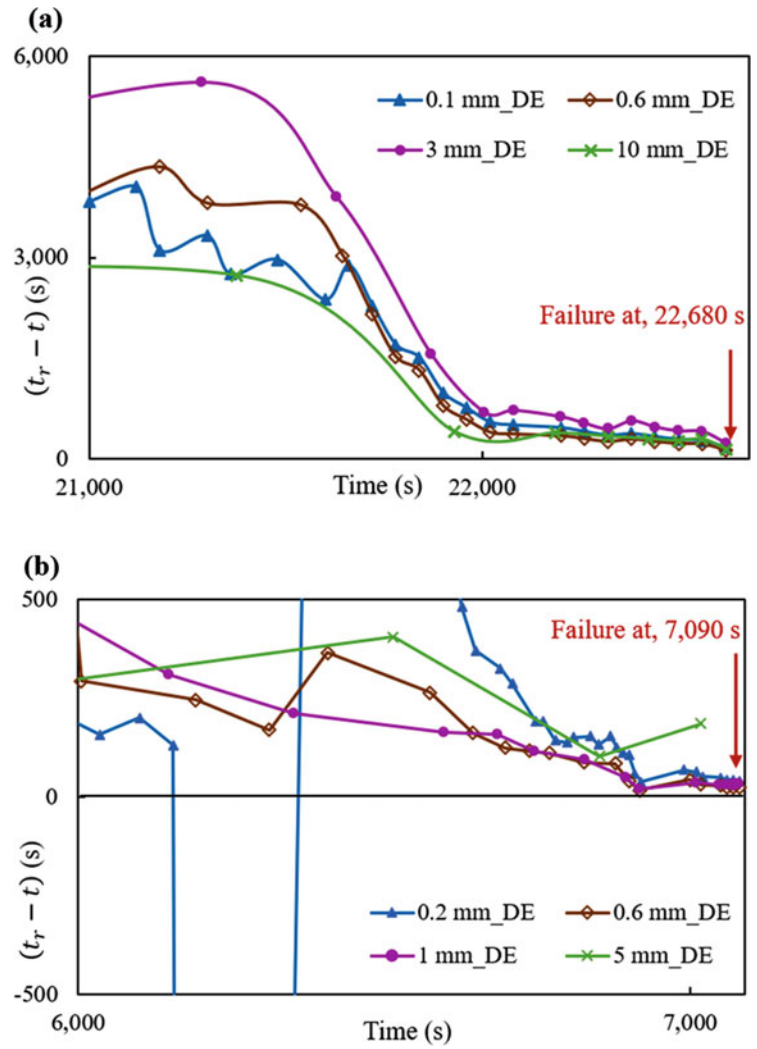
Fig. 17 Time variation of the time remaining to failure $(t_r$-$t)$ by the VAA method using the data processed by the MA method for (**a**) natural slope experiment, Futtsu, and (**b**) in-door small-scale model slope experiment

References

Carlà T, Nolesini T, Solari L et al (2019) Rockfall forecasting and risk management along a major transportation corridor in the Alps through ground-based radar interferometry. Landslides 16:1425–1435. https://doi.org/10.1007/s10346-019-01190-y

Crosta GB, Agliardi F (2003) Failure forecast for large rock slides by surface displacement measurements. Can Geotech J 40:176–119. https://doi.org/10.1139/t02-085

Fukuzono T (1985) A new method for predicting the failure time of a slope. In: Proceedings of 4th international conference and field workshops on landslides, Tokyo, Japan, pp 145–150

Mazzanti P, Bozzano F, Cipriani I, Prestininzi A (2015) New insights into the temporal prediction of landslides by a terrestrial SAR interferometry monitoring case study. Landslides 12:55–58

Moriwaki H, Inokuchi T, Hattanji T, Sassa K, Ochiai H, Wang G (2004) Failure processes in a full-scale landslide experiment using a rainfall simulator. Landslides 1:277–288

Ochiai H, Sasahara K, Koyama Y (2021) Landslide field experiment on a natural slope in Futtsu city, Chiba prefecture, Understanding and reducing landslide disaster risk, pp 169–175

Rose ND, Hungr O (2007) Forecasting potential rock slope failure in open pit mines using the inverse-velocity method. Int J Rock Mech Min 44:308–320

Saito M (1965) Forecasting the time of occurrence of a slope failure. In: Proceedings 6th International Conference on Soil Mechanics and Foundation Eng Montreal, Canada 2, pp 537–541

Varnes DJ (1982) Time-deformation relations in creep to failure of earth materials. In: Proceedings of 7th Southeast Asian Geotechnical Conference 2, pp 107–130

Voight B (1988) A relation to describe rate-dependent material failure. Science 243:200–203

Zhou XP, Liu LJ, Xu C (2020) A modified inverse-velocity method of landslides. Eng Geol 268. https://doi.org/10.1016/j.enggeo.2020.105521